

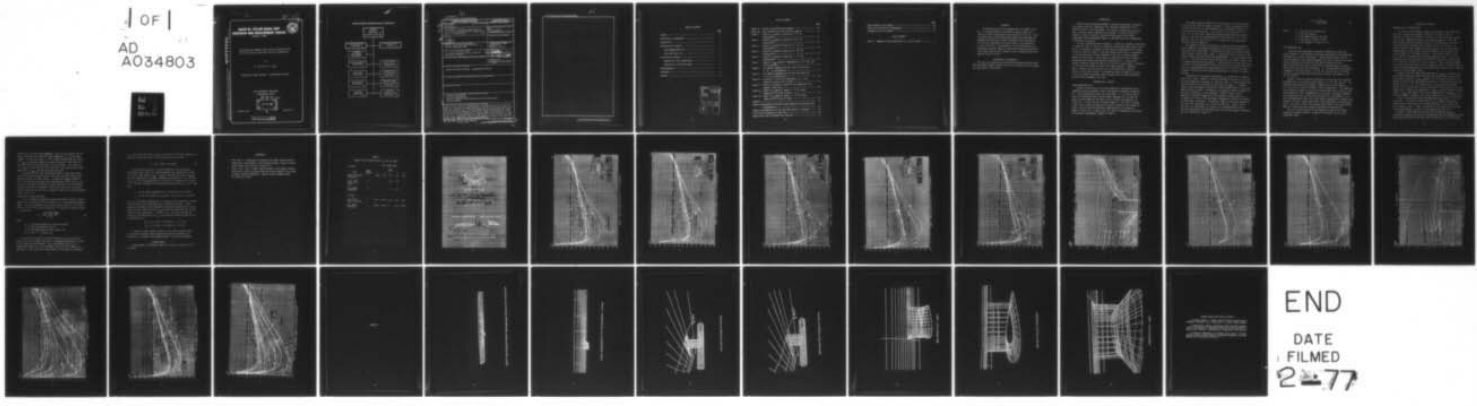
AD-A034 803 DAVID W TAYLOR NAVAL SHIP RESEARCH AND DEVELOPMENT CE--ETC F/8 13/10  
CALCULATIONS OF PRESSURE COEFFICIENTS AND FORCES FOR THE USNS W--ETC(U)  
DEC 76 N M WHITE, H T WANG

UNCLASSIFIED

SPD-740-01

NL

1 OF 1  
AD  
A034803



END  
DATE  
FILMED  
2-77



CALCULATIONS OF PRESSURE COEFFICIENTS AND FORCES FOR THE  
USNS WYMAN WITH AN ADDED STRUT AND FOIL CONFIGURATION

ADA 034803  
SPD-740-01

# DAVID W. TAYLOR NAVAL SHIP RESEARCH AND DEVELOPMENT CENTER

Bethesda, Md. 20084



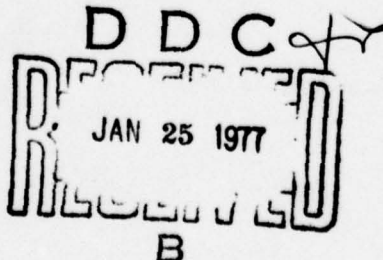
CALCULATIONS OF PRESSURE COEFFICIENTS AND FORCES FOR THE  
USNS WYMAN WITH AN ADDED STRUT AND FOIL CONFIGURATION

by

N.M. White and H.T. Wang

APPROVED FOR PUBLIC RELEASE: DISTRIBUTION UNLIMITED

SHIP PERFORMANCE DEPARTMENT  
DEPARTMENTAL REPORT

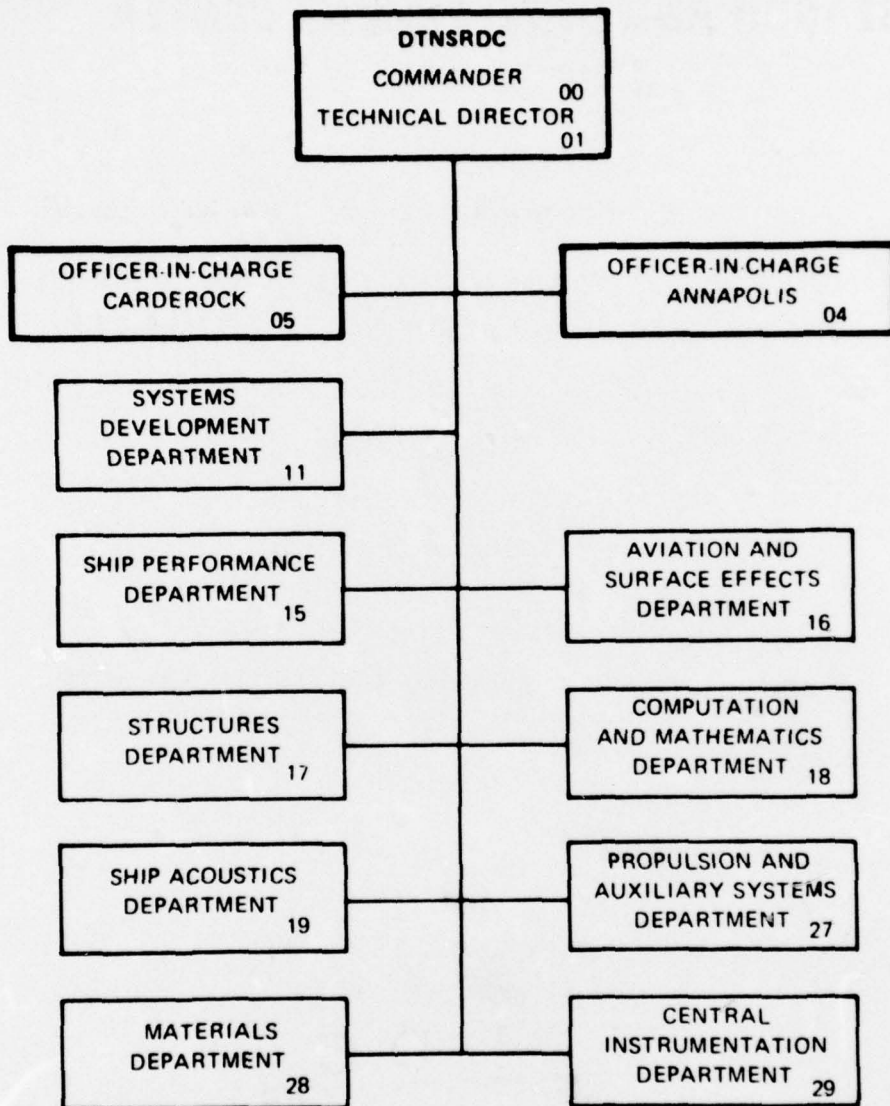


December 1976

SPD-740-01

Copy available to DDC does not  
permit fully legible reproduction

## MAJOR DTNSRDC ORGANIZATIONAL COMPONENTS



UNCLASSIFIED

SECURITY CLASSIFICATION OF THIS PAGE (When Data Entered)

REPORT DOCUMENTATION PAGE		READ INSTRUCTIONS BEFORE COMPLETING FORM
14. REPORT NUMBER SPD-740-01	2. GOVT ACCESSION NO.	3. RECIPIENT'S CATALOG NUMBER
6. TITLE (and Subtitle) Calculations of Pressure Coefficients and Forces for the USNS WYMAN with an Added Strut and Foil Configuration.		5. TYPE OF REPORT & PERIOD COVERED 9. Final rept.,
10. AUTHOR(s) N.M. White H.T. Wang	6. PERFORMING ORG. REPORT NUMBER	
7. PERFORMING ORGANIZATION NAME AND ADDRESS David W. Taylor Naval Ship R&D Center Bethesda, Maryland 20084		8. CONTRACT OR GRANT NUMBER(s) 10. PROGRAM ELEMENT, PROJECT, TASK AREA & WORK UNIT NUMBERS WR N65 197 76 Work Unit 1552-150
11. CONTROLLING OFFICE NAME AND ADDRESS Naval Ship Engineering Center (Code 6136) Washington, DC 20362		12. REPORT DATE 11. December 1976
14. MONITORING AGENCY NAME & ADDRESS (if different from Controlling Office)		13. NUMBER OF PAGES 30 1237P
16. DISTRIBUTION STATEMENT (of this Report)  APPROVED FOR PUBLIC RELEASE: DISTRIBUTION UNLIMITED		15. SECURITY CLASS. (of this report) UNCLASSIFIED
17. DISTRIBUTION STATEMENT (of the abstract entered in Block 20, if different from Report)		
18. SUPPLEMENTARY NOTES		
19. KEY WORDS (Continue on reverse side if necessary and identify by block number) Pressure Distributions Strut-Foil Configuration Numerical Modeling (Two-Dimensional and Three-Dimensional) Cavitation Speed		
20. ABSTRACT (Continue on reverse side if necessary and identify by block number) A selected foil and strut configuration to be added to the hull of the USNS WYMAN was subjected to computer analysis to obtain the force and pressure distributions over the foil. Both two-dimensional and three-dimensional models were developed and compared to obtain both a range of predicted lift coefficients for the given configuration, and the effect of the presence of a strut on the foil. The presence of a strut and non-zero foil pitch angle were both found to have significant effects on the pressure distribution over the foil as well as an effect on the total applied force.		

SECURITY CLASSIFICATION OF THIS PAGE(When Data Entered)

SECURITY CLASSIFICATION OF THIS PAGE(When Data Entered)

## TABLE OF CONTENTS

	<u>Page</u>
ABSTRACT -----	1
ADMINISTRATIVE INFORMATION -----	1
INTRODUCTION -----	2
PRESENTATION OF RESULTS -----	2
THREE-DIMENSIONAL FOIL -----	2
TWO-DIMENSIONAL FOIL -----	4
DISCUSSION OF RESULTS -----	5
PRESSURE AND LIFT COEFFICIENTS -----	5
PREDICTION OF CAVITATION SPEED -----	6
ACKNOWLEDGEMENT -----	7
REFERENCES -----	8
APPENDIX -----	23

ACCESSION FOR	
NTIS	White Section <input checked="" type="checkbox"/>
DDC	Buff Section <input type="checkbox"/>
UNANNOUNCED <input type="checkbox"/>	
JUSTIFICATION .....	
BY .....	
DISTRIBUTION/AVAILABILITY CODES	
DIST.	AVAIL. 300, & SPECIAL
A	

## LIST OF FIGURES

	Page
Figure 1A - Sketch of Ship-Strut-Foil System-----	10
Figure 1B - Sign Convention for Flow and Pitch Angles-----	10
Figure 2 - Graph of $C_p$ Against % Chord for $\beta = 0^\circ$ , 3D Configuration-----	11
Figure 3 - Graph of $C_p$ Against % Chord for $\beta = +2^\circ$ , 3D Configuration-----	12
Figure 4 - Graph of $C_p$ Against % Chord for $\beta = -2^\circ$ , 3D Configuration-----	13
Figure 5 - Graph of $C_p$ Against % Chord for $\beta = +5^\circ$ , 3D Configuration-----	14
Figure 6 - Graph of $C_p$ Against % Chord for $\beta = -5^\circ$ , 3D Configuration-----	15
Figure 7 - Graph of $-C_{p\max}$ Against % Semispan for $\beta = 0^\circ, +2^\circ, +5^\circ$ , 3D Configuration-----	16
Figure 8 - Foil Deeply Submerged and Foil with Flat Plate for $\alpha = 0^\circ$ , 3D Configuration-----	17
Figure 9 - Foil Deeply Submerged and Foil with Flat Plate for $\alpha = +2^\circ$ , 3D Configuration-----	18
Figure 10 - Variation in Local Lift Coefficient, $C_{LL}$ , in the Spanwise Direction, All 3D Cases-----	19
Figure 11 - Graph of $C_p$ Against % Chord for Two Dimensional Foil Beneath a Flat Plate-----	20
Figure 12 - Graph of $C_p$ Against % Chord, $\alpha = 0^\circ$ All Cases, Comparison for 2D And 3D Cases-----	21
Figure 13 - Graph of $C_p$ Against % Chord, $\alpha = +2^\circ$ All Cases, Comparison for 2D and 3D Cases-----	22
APPENDIX -----	23
Graphics Representation of Entire Three-Dimensional Ship-Strut-Foil Configuration-----	24
Graphics Representation of Foil and Strut Section - Enlarged -----	25
Front View of Enlarged Foil and Strut -----	26
Angled Front View of Enlarged Foil and Strut -----	27

	Page
Upper Surface of Foil-Detail-----	28
Side View of Strut-Foil Configuration-----	29
Enlarged View of Foil-Detail-----	30

**LIST OF TABLES**

Table 1 - Summary of Lift Coefficients, $C_L$ , for All Cases-----	9
--	---

## ABSTRACT

A selected foil and strut configuration to be added to the hull of the USNS WYMAN was subjected to computer analysis to obtain the forces and pressure distributions over the foil. Both two-dimensional and three-dimensional models were developed and compared to obtain both a range of predicted lift coefficients for the given configuration, and the effect of the presence of a strut on the foil. The presence of a strut and non-zero foil pitch angle were both found to significantly depress the pressure coefficients over the foil surface as well as increasing the total applied force on the foil.

## ADMINISTRATIVE INFORMATION

This work was sponsored by the Naval Ship Engineering Center under Work Procurement Request #WR-N65-197-76-WR of 30 June 1976 with internal job order number 1-1552-150-01.

## INTRODUCTION

NAVSEC Code 6136 requested DTNSRDC to provide calculations of pressure distributions and lift coefficients on a selected configuration of foil beneath the hull of the USNS WYMAN. The results of calculations are given here in several forms in answer to that request. In order to provide as thorough a study as possible, calculations were made for both three-dimensional and two-dimensional models of the ship-strut-foil configuration illustrated in Figure 1A.

Two foil orientations were considered. In the first instance (illustrated in Figure 1B, CASE 1), the foil is parallel to the ship bottom, and the onset flow is at an angle,  $\beta$ , relative to both the ship bottom and the foil chord. As seen in Figure 1B, CASE 1, a positive angle of onset flow,  $\beta$ , corresponds to the case where the vertical component of the flow is directed upward toward the ship bottom. In this case, the ship plus foil may be viewed as undergoing pitch and/or heave motions in parallel flow. In the second instance (shown in Figure 1B, CASE 2), the foil has a pitch angle,  $\alpha$ , relative to the ship bottom, while the onset flow remains parallel. Figure 1B, CASE 2, defines a positive value of  $\alpha$  as a nose-up pitch of the foil relative to the ship's bottom. The dimensions shown in Figure 1A, as well as the illustrated coordinate system and conventions for angle definition, are those used throughout this study.

## PRESENTATION OF RESULTS

### THREE-DIMENSIONAL FOIL

Pressure coefficients for the three-dimensional configurations were computed by using the Douglas lifting body program, described in Reference (1). The following three cases were calculated: (1) the finite aspect-ratio foil having NACA 0020 sections deeply submerged ( $h \rightarrow \infty$  in Figure 1B, CASE 1) in the absence of the ship or strut at onset flow angles,  $\beta$ , of  $0^\circ$  and  $\pm 2^\circ$ ; (2) the same foil with pitch angles,  $\alpha$ , of  $0^\circ$  and  $\pm 2^\circ$  placed 2 feet (0.61 m) below a horizontal flat plate in parallel flow (Figure 1B, CASE 2), and (3) the ship-strut-foil configuration in its entirety at angles of onset flow,  $\beta$ , equal to  $0^\circ$ ,  $\pm 2^\circ$ , and  $\pm 5^\circ$  simulating pitch or heave of the entire configuration (Figure 1B, CASE 1).

The computed pressure coefficient distributions for various portions of the foil are shown in Figures 2 through 9. These calculations do not include the effect of the ship boundary-layer displacement thickness,  $\delta^*$ , on the pressure distributions. The value of  $\delta^*$  was estimated to be 0.1 feet (0.03 m) which would reduce the clearance between the ship and foil. However, since the actual gap between the ship bottom and foil is everywhere at least two feet (0.61 m), it was assumed that the displacement thickness could be neglected.

The Appendix contains illustrations showing the extent of geometric detail employed in the numerical modeling of the various components of the ship-strut-foil configuration. The modeling was done using digitized data taken directly from the ship's lines. A fine grid was used on the foil and strut sections, with data lines taken approximately 1.3-1.5 feet apart (0.40-0.46 m). A coarser grid was used on the ship since its shape is simple, with an average quadrilateral being about 1.3 feet wide and 26.5 feet long (0.40 x 8.08 m). At the intersection of the strut with the hull and the strut with the foil, quadrilaterals were spaced about every 0.5 ft (0.15 m) in each direction, allowing for more accurate calculations at the areas of maximum interest.

Information on the pressure coefficients,  $C_p$ , on the foil is supplied here in five forms. Figures 2-6 show the chordwise distributions of  $C_p$  for the three-dimensional equivalent of Figure 1B, CASE 1, at three spanwise foil locations relative to the strut for five onset flow angles  $\beta$ . Secondly, Figure 7 shows the spanwise distribution of the minimum values of  $C_p$  on the upper and lower surfaces. In addition, the changing chordwise location of the line of minimum  $C_p$  is also indicated. Thirdly, Figures 8 and 9 respectively provide a comparison of the chordwise distributions of  $C_p$  at angles  $\alpha$  of  $0^\circ$  and  $+2^\circ$  for the deeply submerged foil and the foil placed two feet below a flat plate. In addition, Figure 10 illustrates changes in the local lift coefficient,  $C_{LL}$ , across the foil span. Lastly, Table 1 gives the lift coefficient,  $C_L$ , which is the integrated effect of the pressure coefficients, for the three cases at the various angles considered. The lift coefficient is given by

$$C_L = \frac{L}{(1/2)\rho U^2 C(2S)} \quad [1]$$

where            L is the lift on the entire foil  
                  $\rho$  is the fluid density  
                 U is the advance speed of the ship  
                 C is the chord = 10 feet (3.05 m)  
                 S is the semispan = 15 feet (4.57 m)

#### TWO-DIMENSIONAL FOIL

Since the three-dimensional lifting body program has seldom been used at DTNSRDC, it was decided to make some calculations on two-dimensional configurations to check its accuracy. These calculations were made by using the potential flow computer program XYPF, which is based on the theory given in Reference (2) with corrections made to provide for lift. Modifications were also made to allow for a horizontal plane of symmetry. The following two cases were calculated: (1) the NACA 0020 section deeply-submerged at foil pitch angles,  $\alpha$ , of  $0^\circ$ ,  $\pm 2^\circ$ , and  $\pm 5^\circ$ , and (2) the same section placed two feet below a flat plate with foil pitch angles,  $\alpha$ , of  $0^\circ$ ,  $\pm 2^\circ$ , and  $\pm 5^\circ$ .

Figure 11 shows the pressure coefficients for the case of the section submerged below a flat plate at pitch angles,  $\alpha$ , of  $0^\circ$ ,  $\pm 2^\circ$ , and  $\pm 5^\circ$ . The pressure coefficients for the deeply submerged foil at pitch angles,  $\alpha$ , of  $0^\circ$  and  $2^\circ$  may be found in Figures 12 and 13 respectively. For comparison, also included in Figures 12 and 13 are the equivalent cases of the two- and three-dimensional foils submerged below a flat plate, the deeply submerged three-dimensional foil, and the full ship-strut-foil configuration. For the three-dimensional cases, the results shown correspond to a location near midspan of the foil, where results most closely approximate two-dimensional cases. For clarity, some of the pressure coefficients on the lower surface which are similar for cases already illustrated have been omitted.

The lift coefficients for the two-dimensional cases for all angles considered are shown in Table 1, along with the results for the three-dimensional cases.

## DISCUSSION OF RESULTS

### PRESSURE AND LIFT COEFFICIENTS

For the cases illustrating a change in pitch angle of the rigid ship-strut-foil configuration (Figures 2 through 6), the onset flow is essentially forced to be parallel to the foil and ship bottom when passing over the foil, regardless of the initial angle of approach. Thus, the force increase due to the change in pitch is relatively small (see Table 1), increasing about 60 percent over the range of  $0^\circ$  to  $+5^\circ$  of pitch. In contrast, when the foil changes its position relative to the hull bottom (approximated by a flat plate), the force increases over 100 percent for a pitch change of  $+2^\circ$  as shown in Table 1. This drastic change is born out in both the two-dimensional and three-dimensional cases. For the two-dimensional case, the  $C_p$  value for the  $+5^\circ$  pitch angle has a minimum value of -3.2 which is off the scale shown in Figure 11. These large  $C_p$  changes in the flat plate cases are due to the cumulative effects of positive angle of foil pitch and the presence of the flat plate, both of which tend to lower the values of  $C_p$  on the upper surface.

Figure 7 shows the location and magnitude of  $-C_{p\max}$  for the upper and lower surfaces along the span of the foil for various angles of onset flow. The chordwise location of  $-C_{p\max}$  changes from 17.5 percent of chord to 22.5 percent of chord on the upper surface of the foil as the angle of onset flow changes from  $0^\circ$  to  $+5^\circ$ . The largest value of  $-C_{p\max}$  occurs immediately inboard of the intersection of the foil and strut. The presence of the strut significantly increases the magnitudes of  $-C_{p\max}$  at the strut relative to the value of  $-C_{p\max}$  near midspan. This can be seen readily by comparison of  $C_p$  values in Figures 2 through 6 at foil span locations of  $y/s = 0.33$  and  $0.047$ .

Figure 10 illustrates further the magnitude of the effect of the strut on the foil. The local lift coefficient,  $C_{LL}$ , is markedly lower on the outboard side of the strut, and the smooth decrease in lift, seen in the cases without a strut, is gone. In addition, as the angle of pitch becomes increasingly negative,  $C_{LL}$  can be driven negative near the tip.

Figures 12 and 13 show very clearly the differences in pressure coefficient  $C_p$  between the various two-dimensional and three-dimensional cases. Both figures show that on the lower side, the values of  $C_p$  for the various

cases are in relatively good agreement. Also, in both figures, the two deeply submerged cases yield the lowest magnitudes of  $C_p$  on the upper surface. At the pitch angle,  $\alpha$ , of  $0^\circ$ , Figure 12 shows that the values of  $-C_{p_{\max}}$  on the upper surface are within 10 percent of each other for the ship-strut-foil case and the two flat plate cases. For a pitch of  $+2^\circ$ , Figure 13 shows that the flat plate cases have significantly larger magnitudes of  $-C_{p_{\max}}$  than the ship-strut-foil case.

In conclusion, the strut intersection exerts a significant effect on the flow over the upper surface of the foil, while not significantly affecting flow on the lower surface. In addition, change in angle of pitch of the entire ship-strut-foil system does not affect the  $C_p$  on the foil nearly as much as rotation of the foil relative to the hull bottom. Rotation of the foil with respect to the ship's hull has a significant effect on the flow over the foil's surfaces as well as on the total applied forces on the foil.

#### PREDICTION OF CAVITATION SPEED

It is of interest to compute the maximum theoretical speed at which a smooth foil may operate free of cavitation, i.e., the cavitation inception speed. With the assumption that cavitation begins when the local static pressure is equal to the vapor pressure  $p_v$ , the cavitation inception speed  $v_I$  is given by

$$v_I = \sqrt{\frac{p_v - (p_0 + \rho gh)}{\frac{1}{2} \rho C_{pm}}} \quad [2]$$

where

$p_0$  is the static pressure at the ocean surface,

$g$  is the acceleration of gravity

$h$  is the depth below the free surface, and

$C_{pm}$  is the ~~minimum~~ value of  $C_p$ .

For the ship-strut-foil case, the minimum value of  $C_p$  on the foil always occurs on its upper side, which is submerged approximately 17 feet (5.18 m) below the free surface. Also, the minimum value of  $C_p$  is approximately equal to  $-1.4$  in the range  $-5^\circ \leq \beta \leq +5^\circ$  (See Figures 2-6). Assuming  $\rho = 1.99 \text{ lb-sec}^2/\text{ft}^4$  ( $1025.6 \text{ kg/m}^3$ ) for the density of seawater,

$p_o = 2160 \text{ lb/ft}^2$  ( $5224 \text{ N/m}^2$ ), and  $p_v = 30 \text{ lb/ft}^2$  ( $72.59 \text{ N/m}^2$ ), Equation [2] yields the following value of  $V_I$  for the ship-strut-foil case

$$V_I = 48.1 \text{ ft/sec} = 28.5 \text{ knots} \quad [3]$$

For cases where the foil is rotated relative to the ship bottom, considerably lower values of  $V_I$  may be expected for large positive values of  $\alpha$  due to lower values of  $C_{pm}$ . Figure 9 shows that the value of  $C_{pm}$  for the three-dimensional foil deeply submerged and pitched at  $2^\circ$  is -0.87 and the  $C_{pm}$  for the three-dimensional foil pitched at  $2^\circ$  beneath a flat plate is -1.49. The use of Equation [2] yields the following values for  $V_I$  for these cases:

$$V_I \text{ for the deeply submerged foil} = 60.98 \text{ ft/sec} = 36.13 \text{ knots}$$

$$V_I \text{ for the foil beneath a flat plate} = 46.60 \text{ ft/sec} = 27.61 \text{ knots}$$

The  $V_I$  for the deeply submerged foil is obviously a most optimistic estimate since the effect of the ship and strut is neglected entirely. A more conservative estimate can be obtained by using the two-dimensional results. Figure 11 shows that the values of  $C_{pm}$  for the two-dimensional foil pitched  $+2^\circ$  and  $+5^\circ$  are respectively -1.82 and -3.19. The use of Equation [2] yields the following values for  $V_{2D}$ , the cavitation inception speed for the two-dimensional foil

$$V_{2D} = 42.2 \text{ ft/sec} = 25.0 \text{ knots at } \alpha = +2^\circ \quad (4a)$$

$$V_{2D} = 31.8 \text{ ft/sec} = 18.9 \text{ knots at } \alpha = +5^\circ \quad (4b)$$

It should be noted, however, that all of the above computed values of cavitation inception speed include no provision for manufacturing inaccuracies or roughness could degrade overall cavitation performance.

#### ACKNOWLEDGEMENT

Acknowledgement is gratefully made to Mr. Charles W. Dawson for his assistance.

#### REFERENCES

1. Hess, John L., "Calculation of Potential Flow About Arbitrary Three-Dimensional Lifting Bodies," Final Technical Report, Douglas Aircraft Company Report #MDC J56-79-01, October 1972.
2. Smith, A.M.O., and J. Pierce, "Exact Solution of the Neumann Problem. Calculation of Non-Circulatory Plane and Axially Symmetric Flows About or Within Arbitrary Boundaries," Douglas Aircraft Company Report #ES-26988, April 1958.

TABLE 1

Summary of Lift Coefficients,  $C_L$ , For All Cases

3D Cases		Angle Varied	Lift Coefficient $C_L$				
Case	Angle		-5	-2	0	+2	+5
Ship-Foil-Strut Combination	$\beta$		0.055	0.10	0.14	0.17	0.22
Foil 2 Feet Below Flat Plate	$\alpha$				0.19	0.44	
Foil Deeply Submerged	$\beta$				0	0.13	

2D Cases							
Foil 2 Feet Below Flat Plate	$\alpha$	-0.65	-0.09	0.34	0.81	1.58	
Foil Deeply Submerged	$\beta$	-0.681	-0.273	0	0.273	0.681	

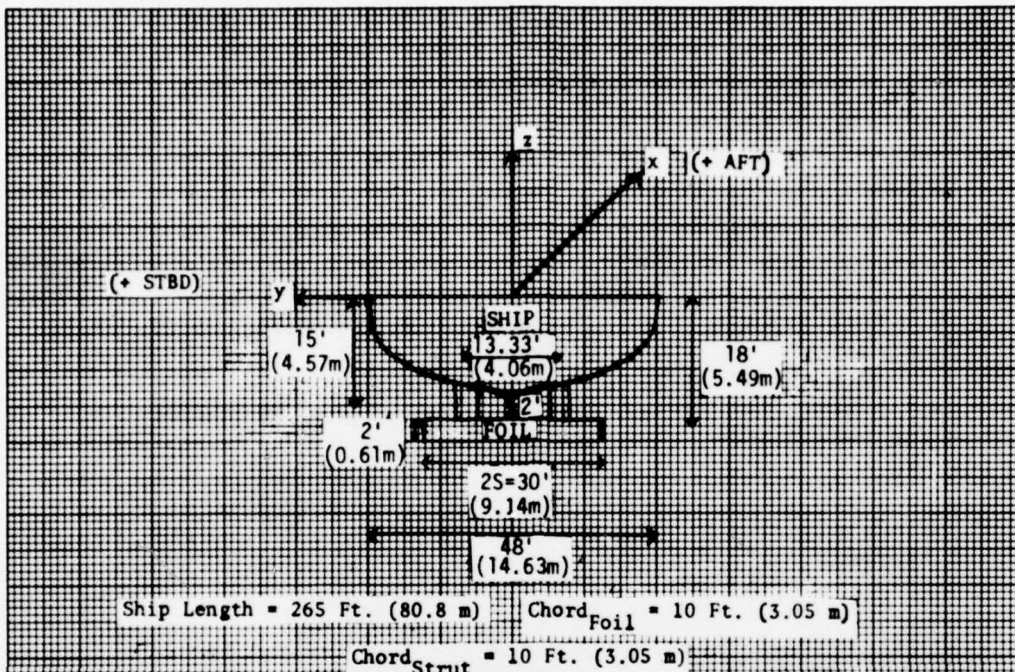


Figure 1A - Sketch of Ship-strut-foil System  
 (Note: Use for relative dimensions only -  
 does not model ship lines)

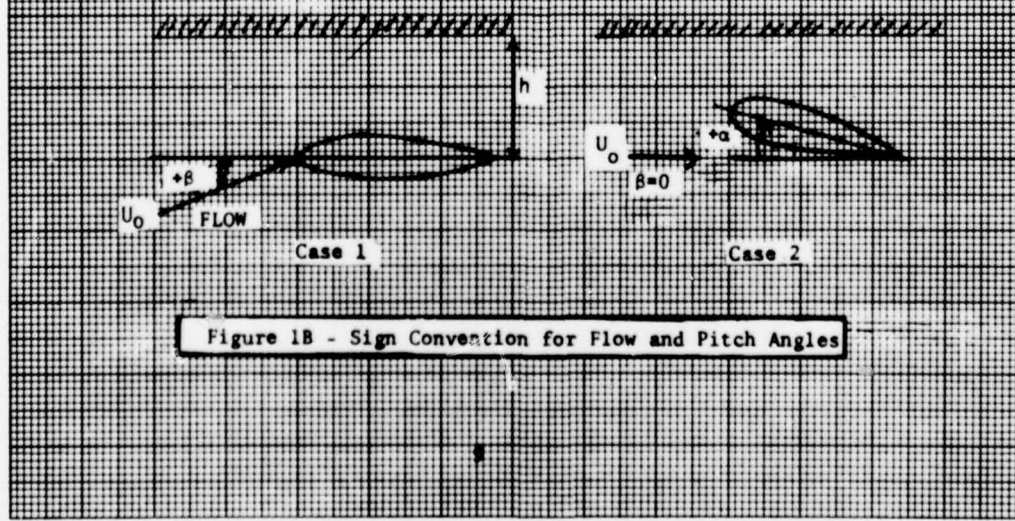


Figure 1B - Sign Convention for Flow and Pitch Angles

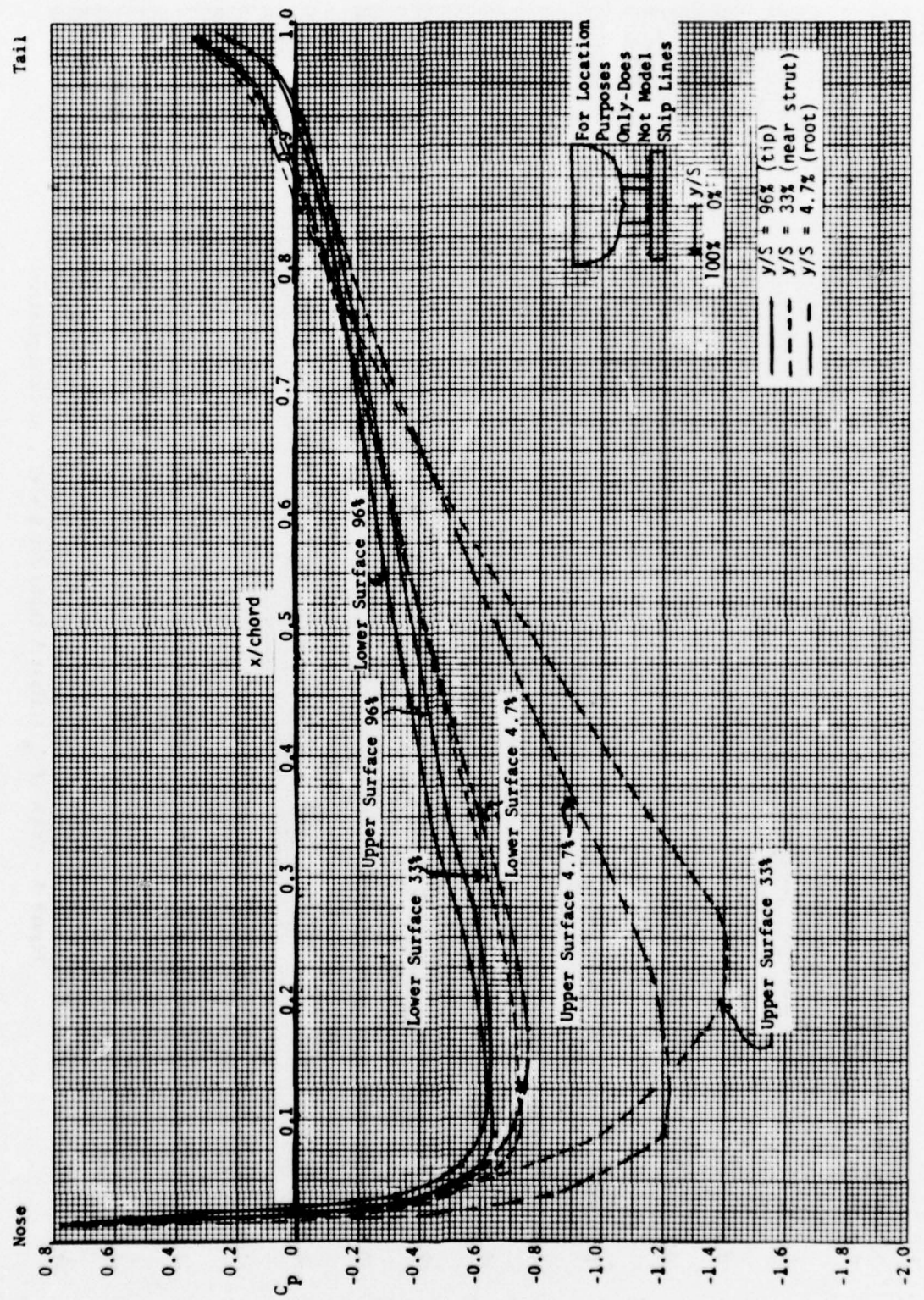


Figure 2 - Graph of  $C_p$  Against  $\frac{x}{\text{chord}}$  for  $\beta = 0$ , 3D Configuration

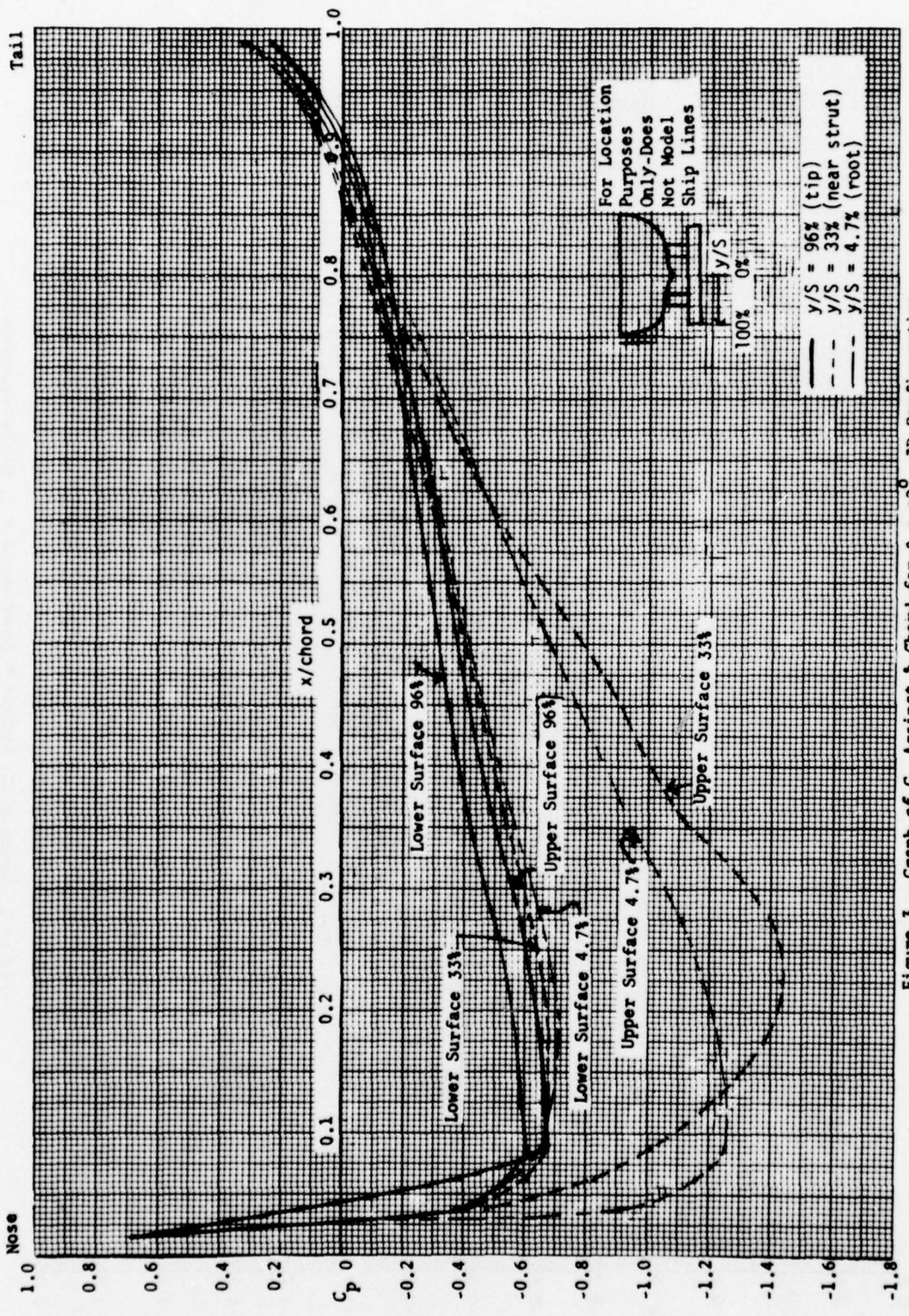


Figure 3 - Graph of  $C_p$  Against % Chord for  $\beta = +2^\circ$ , 3D Configuration

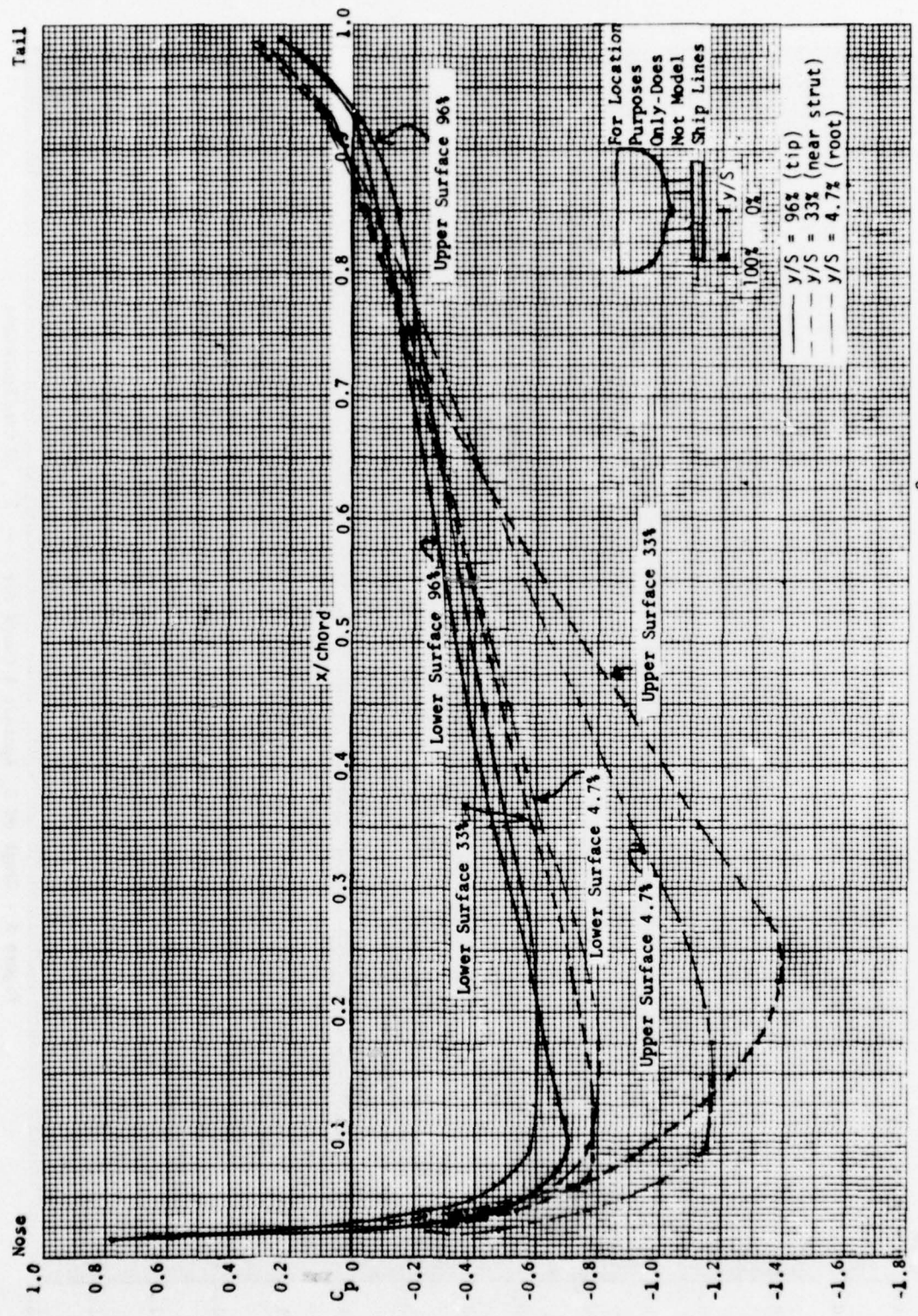


Figure 4 - Graph of  $C_p$  Against  $x/\text{chord}$  for  $\theta = -2^\circ$ , 3D Configuration

Tail

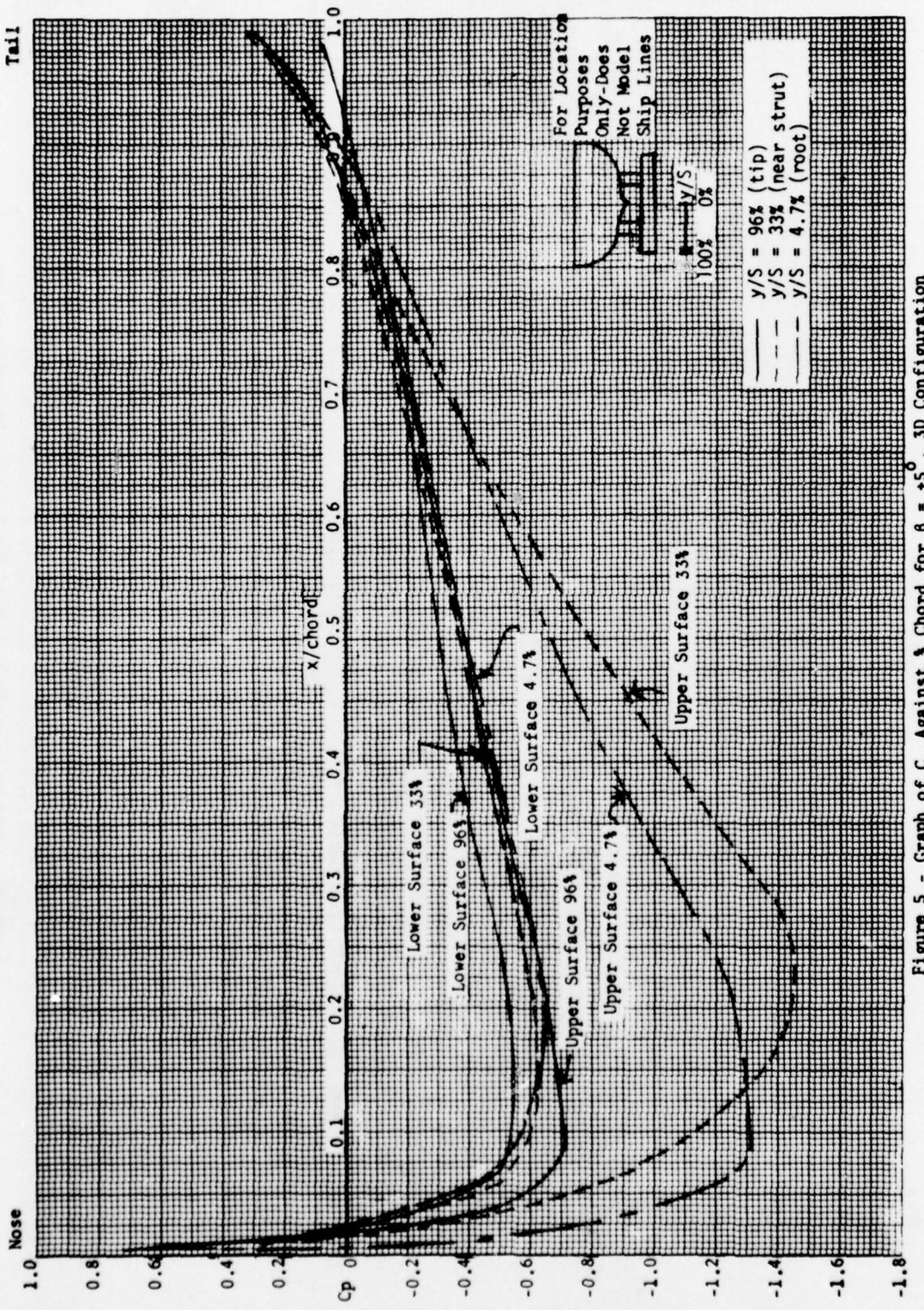


Figure 5 - Graph of  $C_p$  Against  $\frac{x}{\text{chord}}$  for  $\beta = +5^\circ$ , 3D Configuration

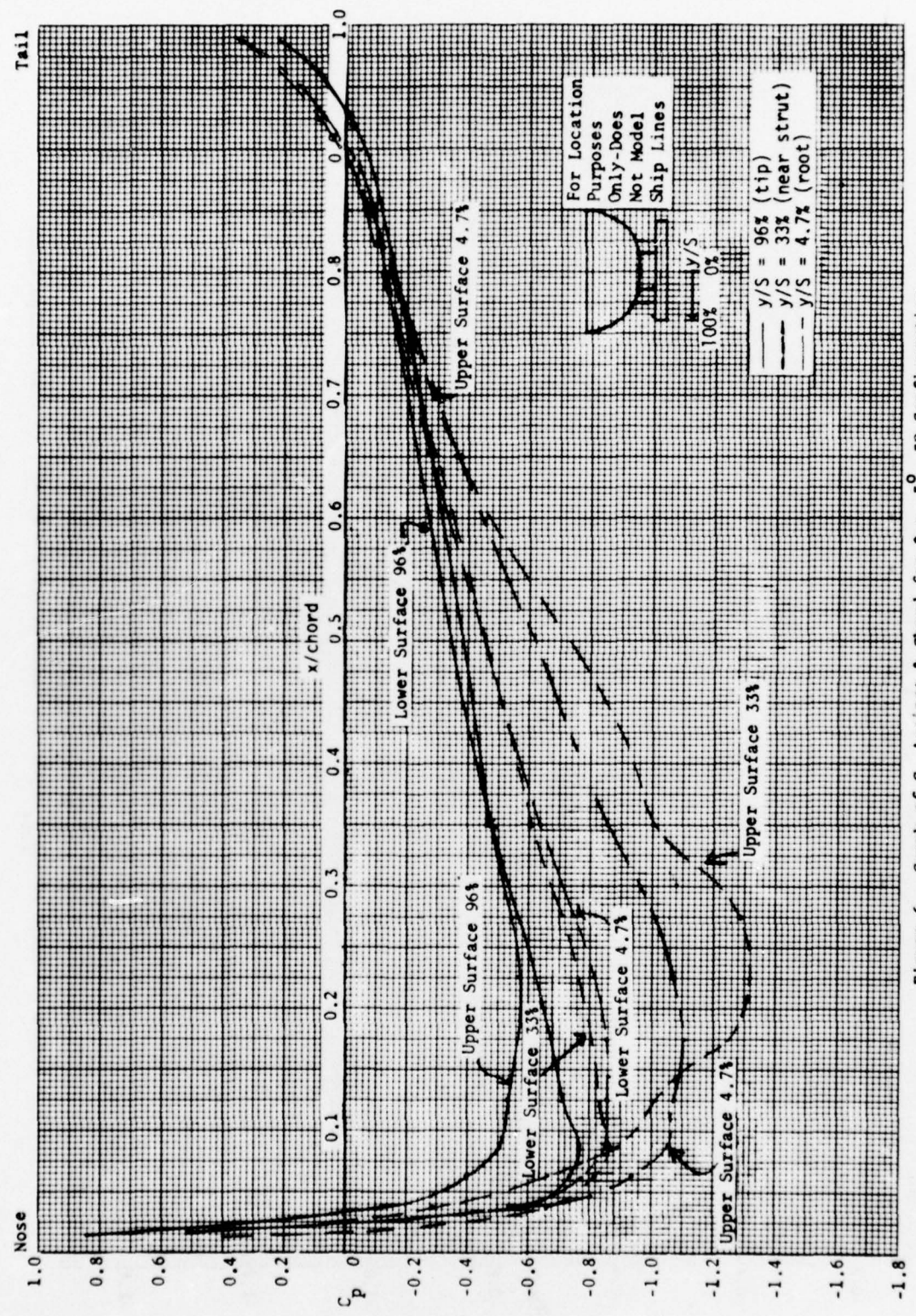


Figure 6 - Graph of  $C_p$  Against % Chord for  $\theta = -5^\circ$ , 3D Configuration

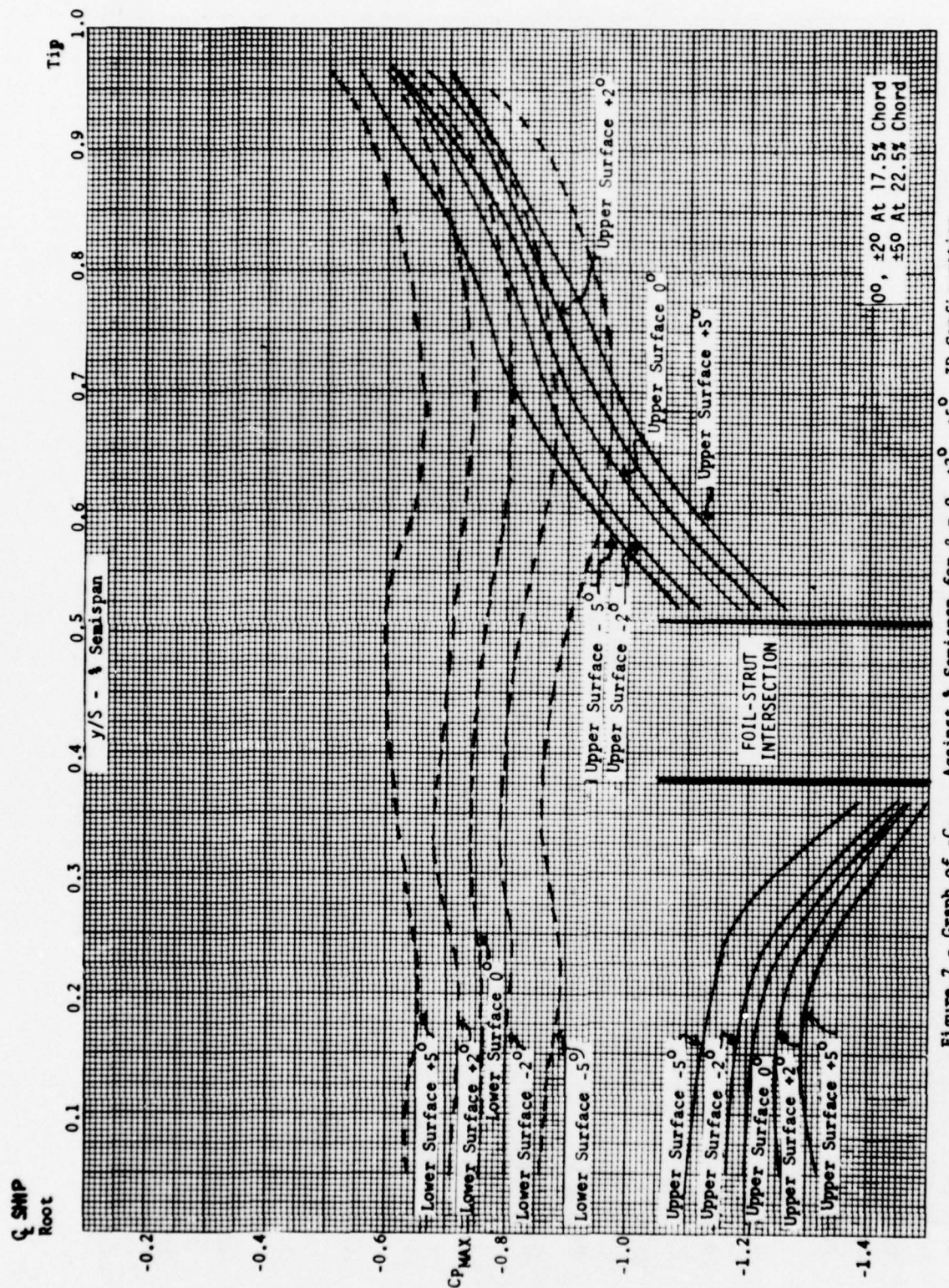


Figure 7 - Graph of  $-C_{p\max}$  Against  $\frac{1}{4}$  Semispan for  $\beta = 0, \pm 2^\circ, \pm 5^\circ, \pm 10^\circ$  At 17.5% Chord

$0^\circ, \pm 2^\circ$  At 17.5% Chord  
 $\pm 5^\circ$  At 22.5% Chord

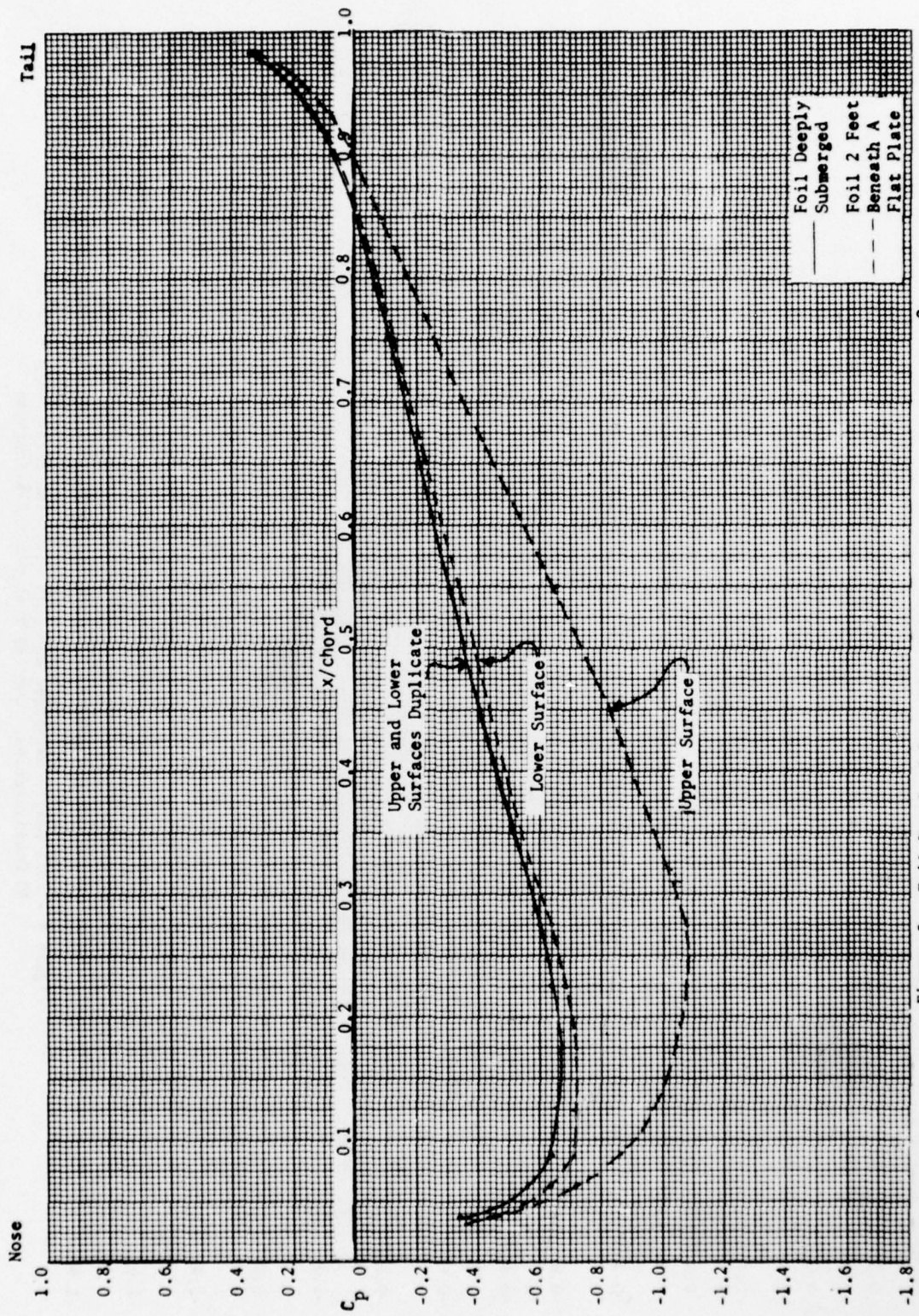


Figure 8 - Foil Deeply Submerged and Foil with Flat Plate for  $\alpha = 0^\circ$ ,  
3D Configuration. Cut Taken at  $y/s = 13\%$  Semispan

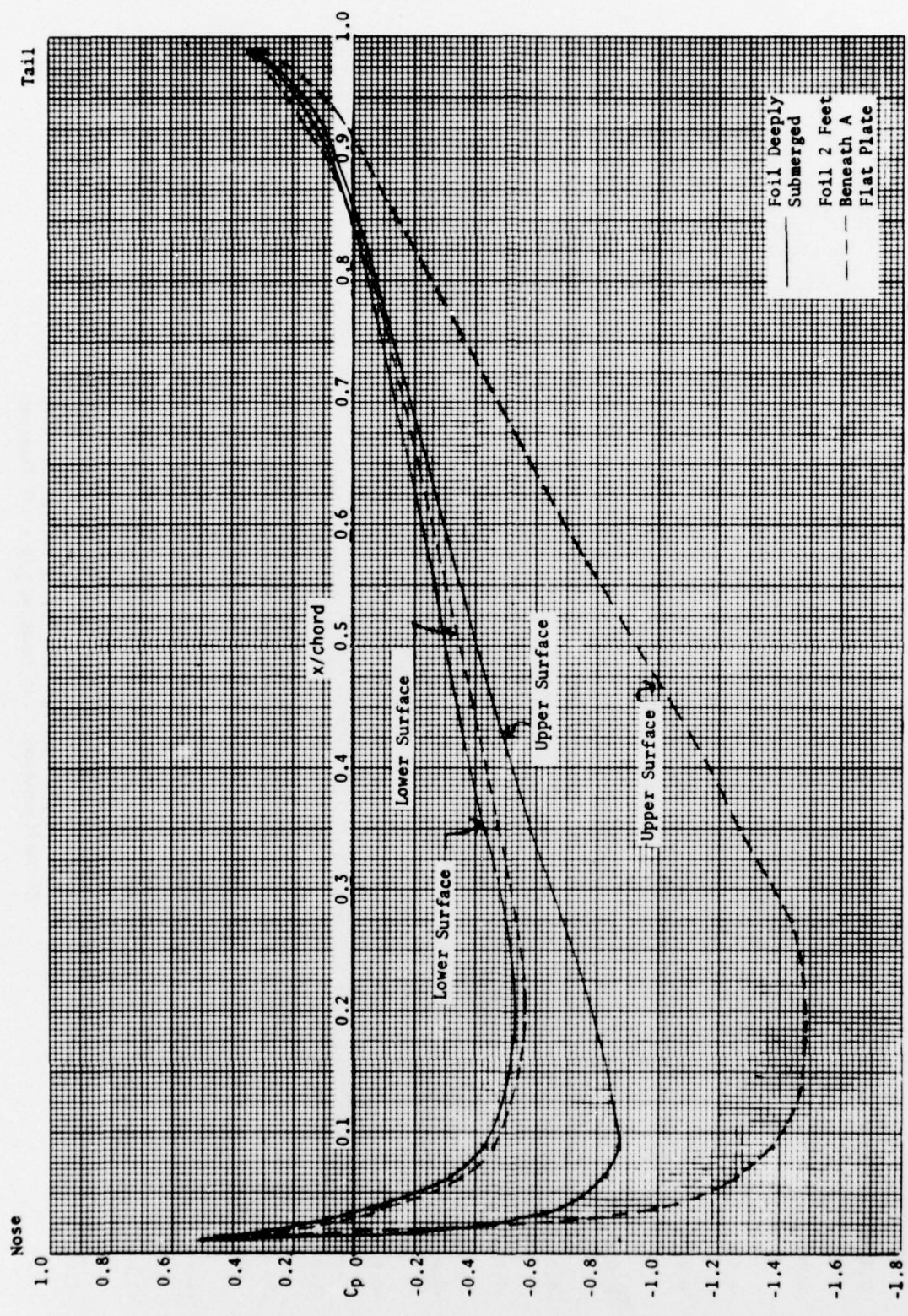
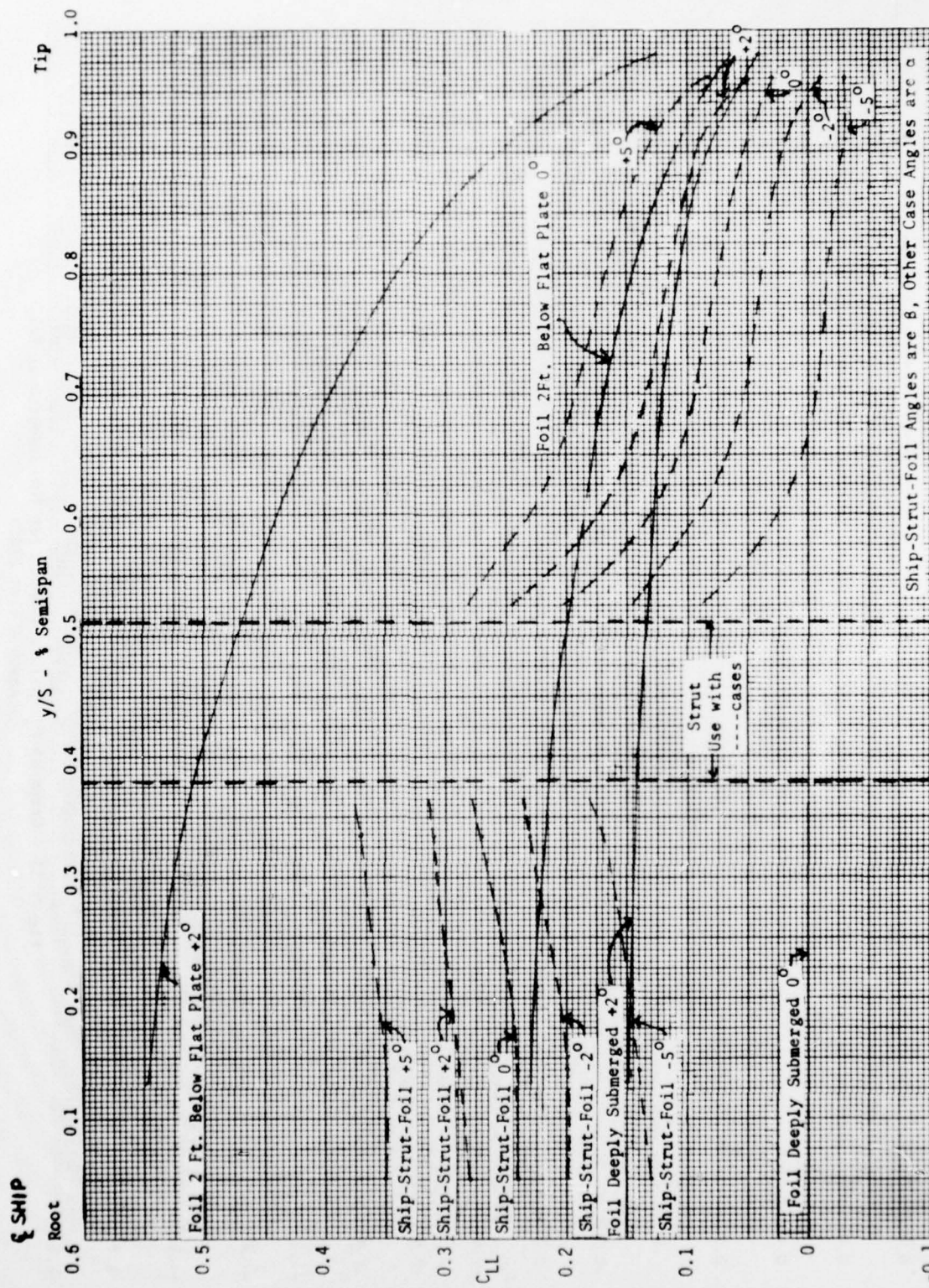


Figure 9 - Foil Deeply Submerged and Foil with Flat Plate for  $\alpha = +2^\circ$ ,  
3D Configuration. Cut Taken at  $y/s = 13\%$  Semispan



-0.1

Ship-Strut-Foil Angles are 8, Other Case Angles are a

Figure 10 - Variation in Local Lift Coefficient,  $C_{LL}$ , in the Spanwise Direction - All 3D Cases

Nose  
Tail

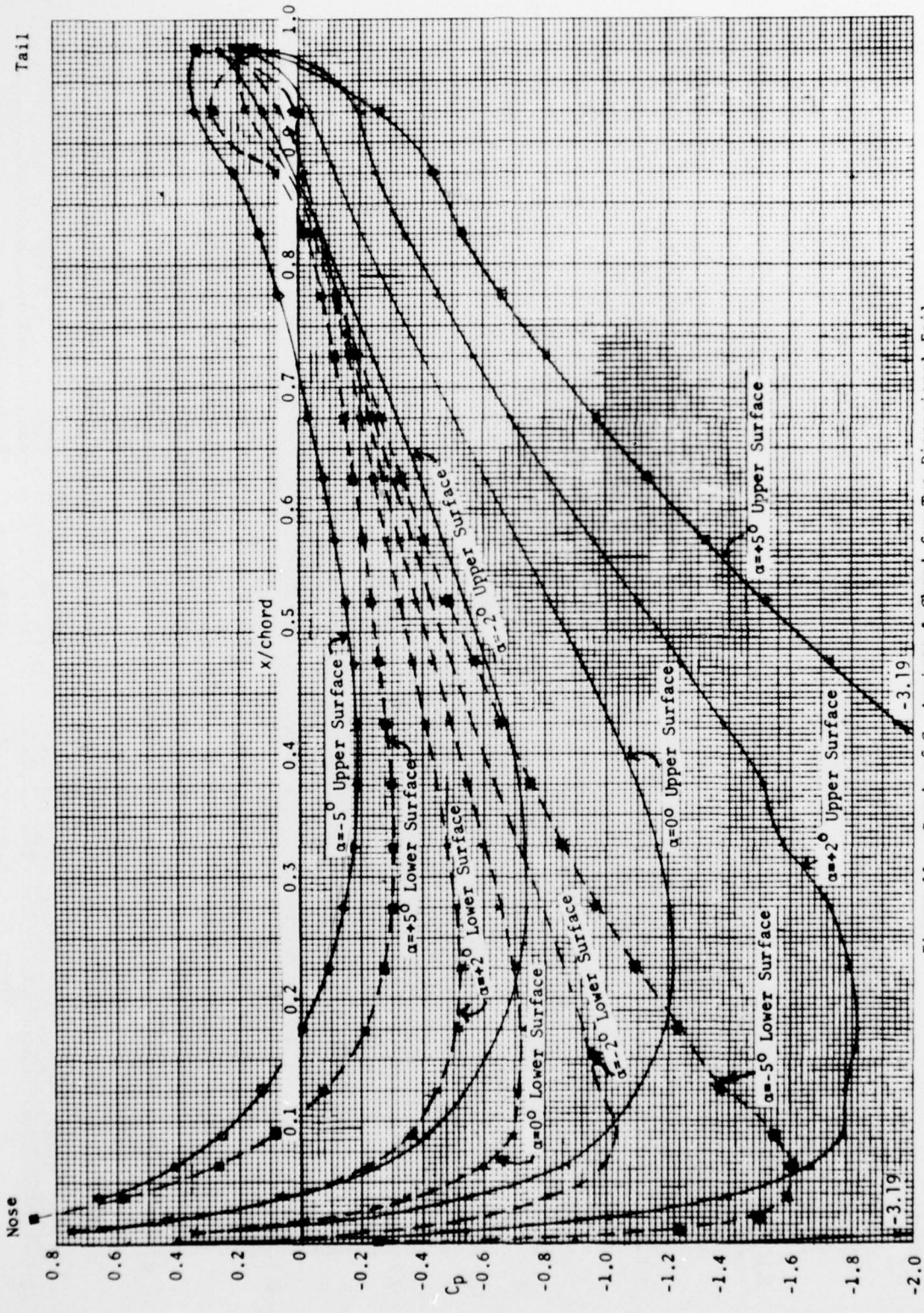


Figure 11 - Graph of  $C_p$  Against  $\frac{x}{\text{chord}}$  for Two-Dimensional Foil Beneath a Flat Plate

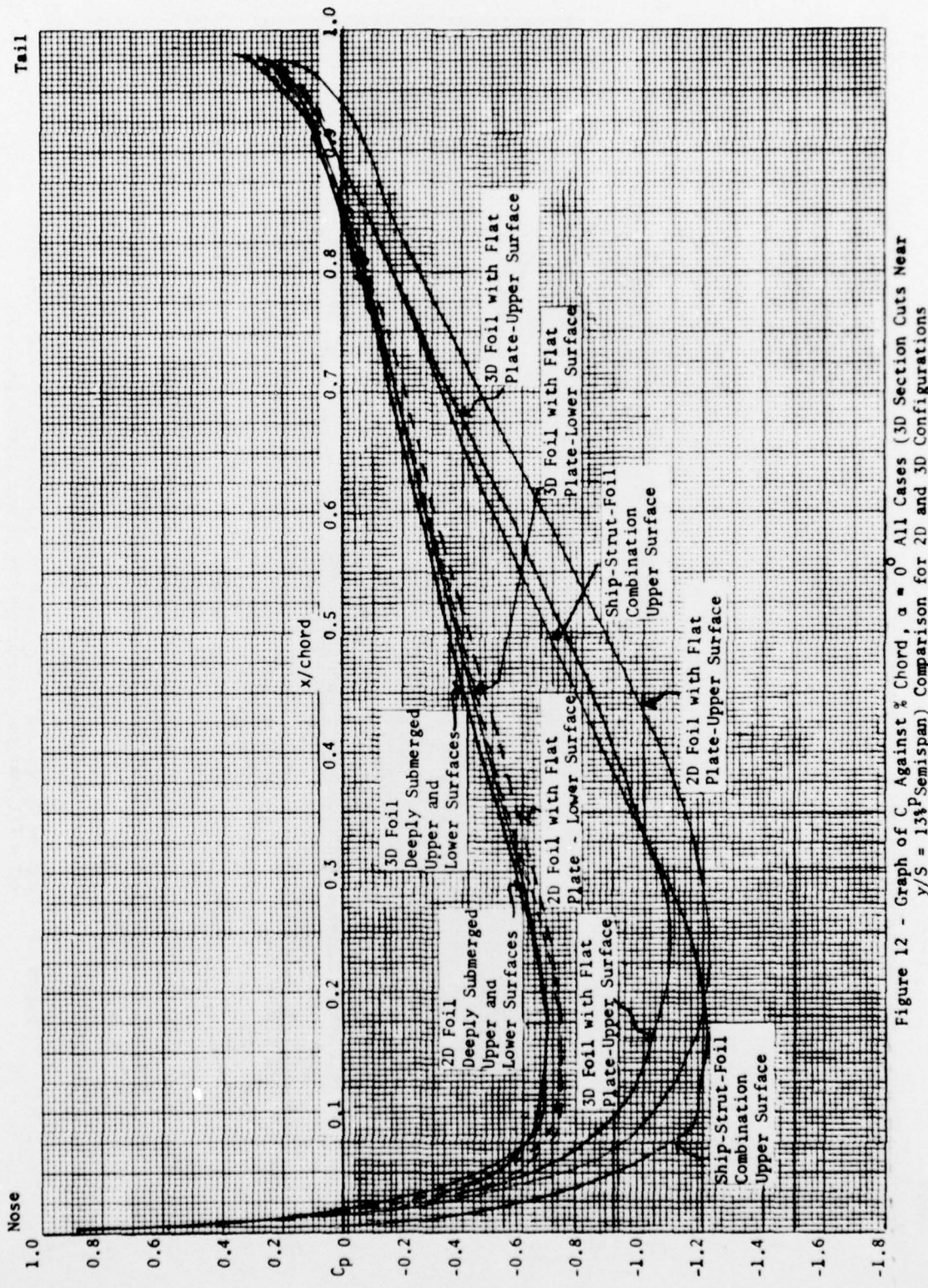


Figure 12 - Graph of  $C_p$  Against % Chord,  $\alpha = 0^\circ$  All Cases (3D Section Cuts Near  $y/S = 13\frac{1}{3}P_{\text{Semispan}}$ ) Comparison for 2D and 3D Configurations

Tail

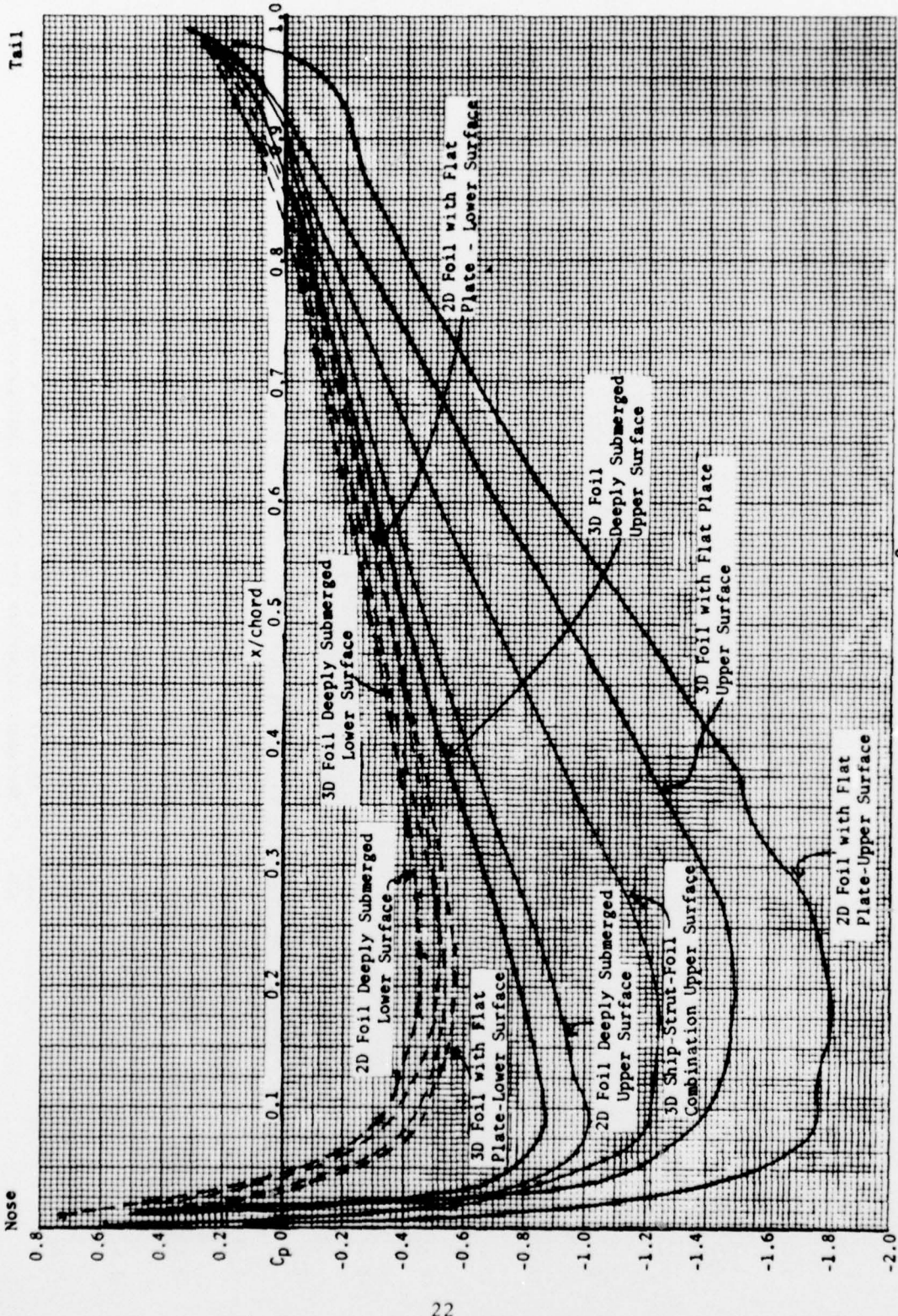


Figure 13 - Graph of  $C_p$  Against  $\frac{x}{\text{Chord}}$ ,  $\alpha = +2^\circ$  All Cases (3D Section Cuts Near  $y/S = 13\%$  Semispan) Comparison for 2D and 3D Configurations

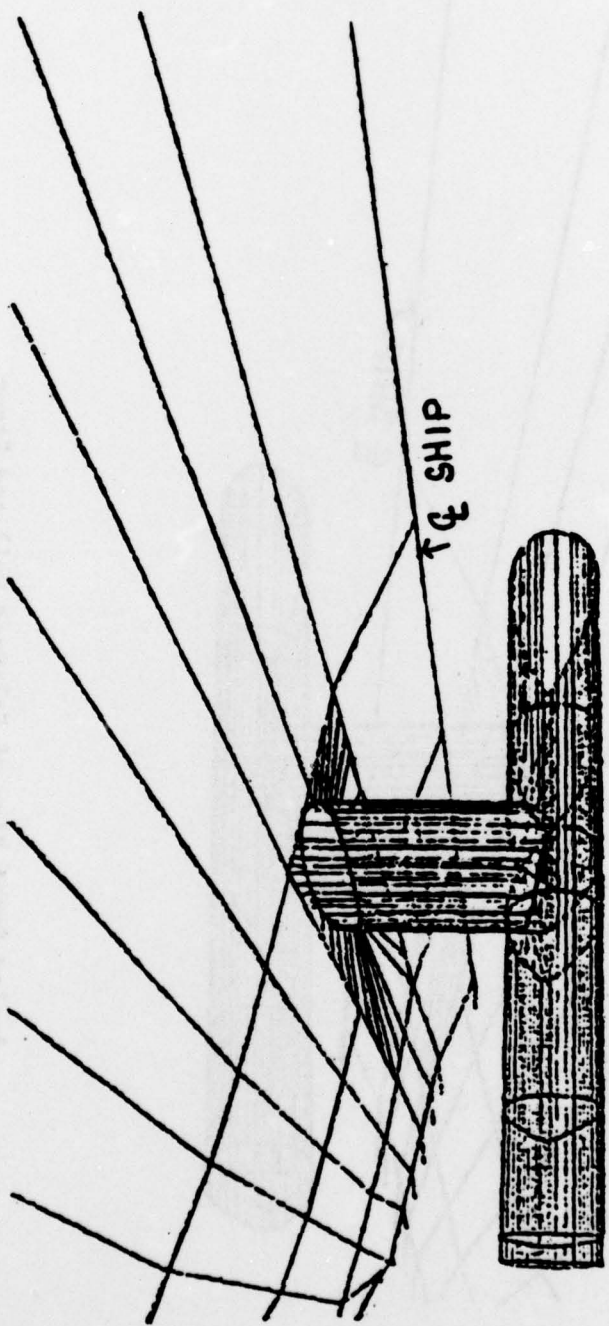
**APPENDIX**

**Graphics Representation of Entire Three-Dimensional Ship-Strut-Foil Configuration**

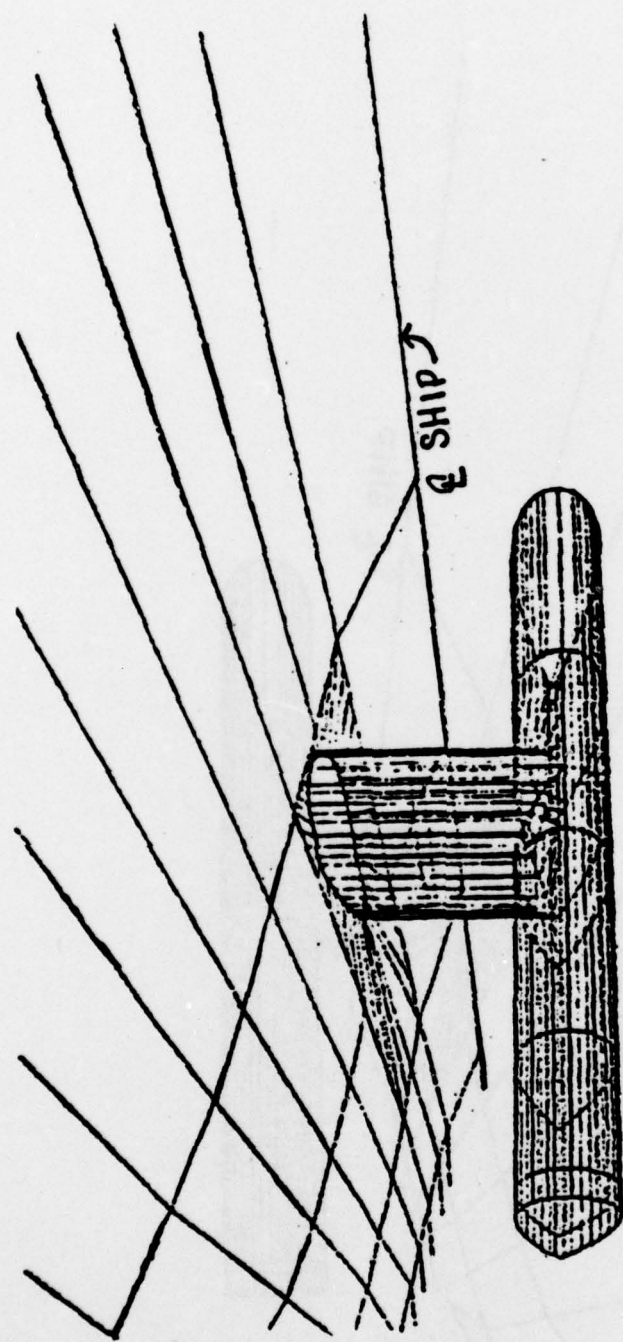


Graphics Representation of Foil and Strut Section - Enlarged



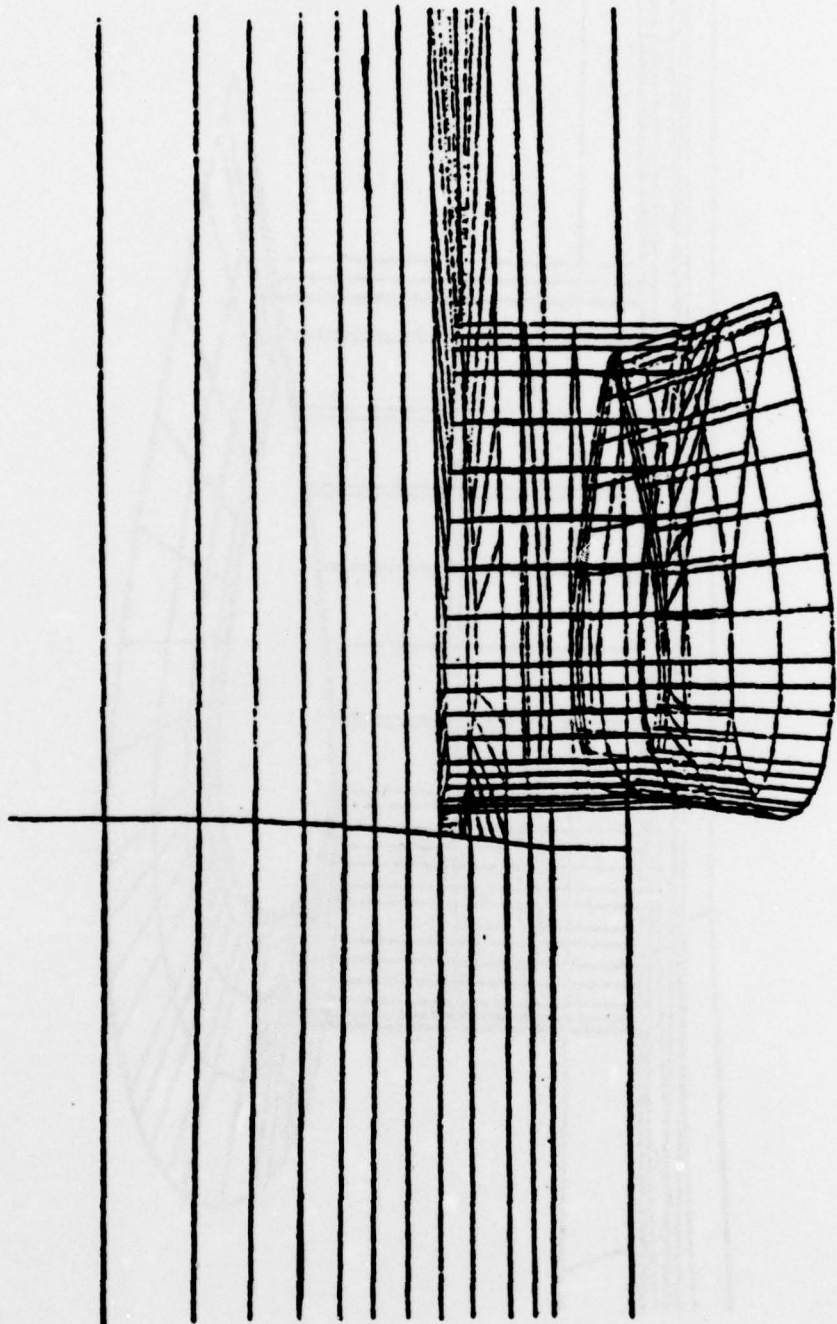


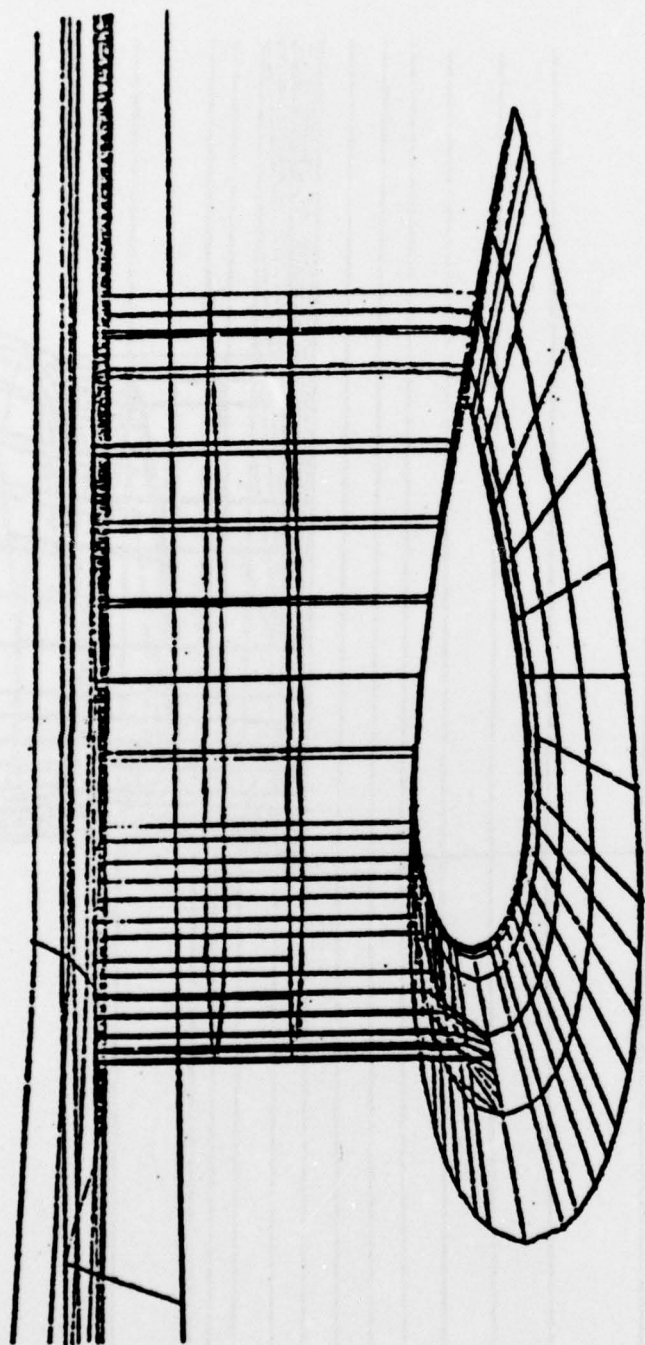
Front View of Enlarged Foil and Strut



Angled Front View of Enlarged Foil and Strut

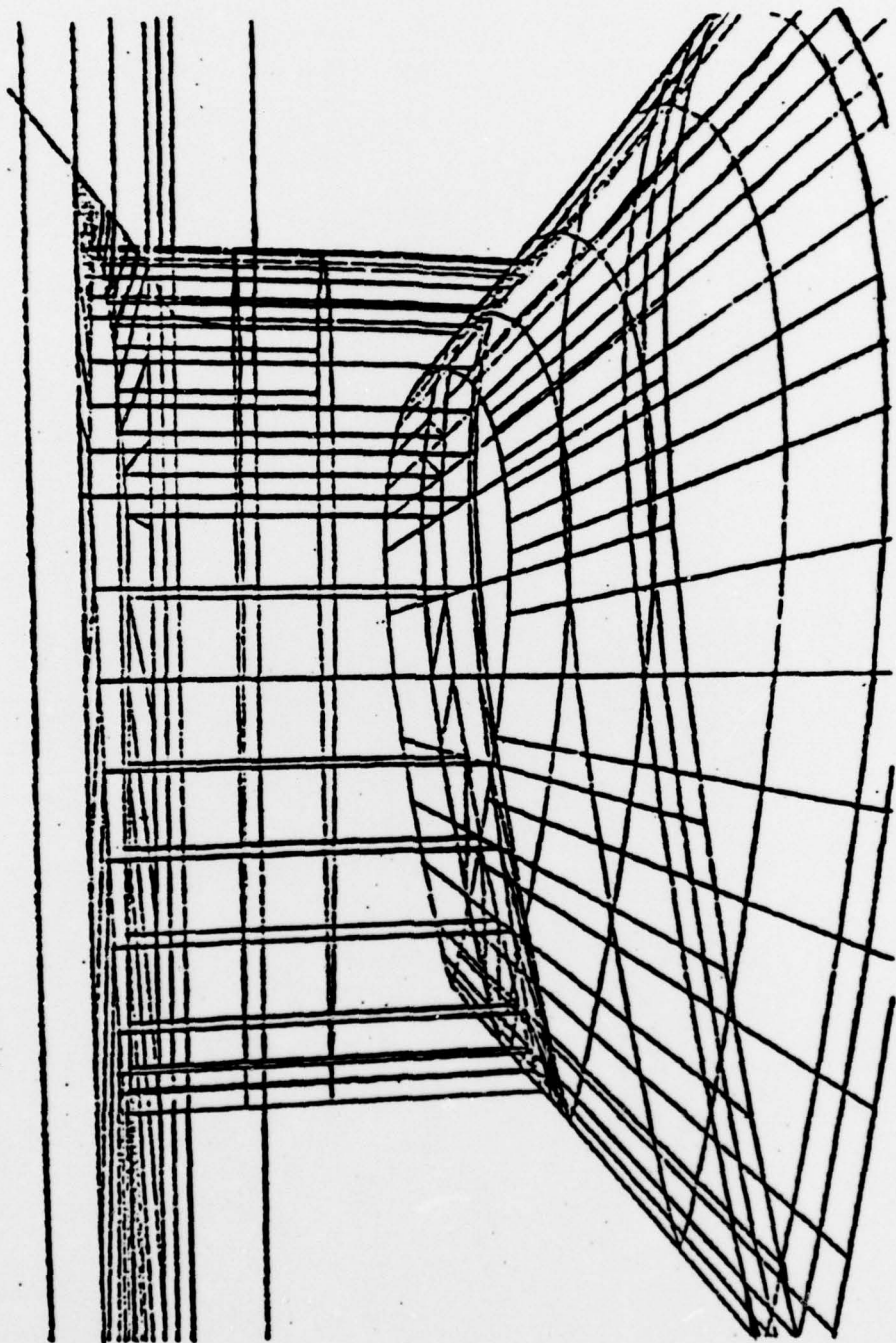
Upper Surface of Foil - Detail





Side View of Strut-Foil Configuration

Enlarged View of Fig 1 - Detail



**DTNSRDC ISSUES THREE TYPES OF REPORTS**

- (1) DTNSRDC REPORTS, A FORMAL SERIES PUBLISHING INFORMATION OF PERMANENT TECHNICAL VALUE, DESIGNATED BY A SERIAL REPORT NUMBER.**
- (2) DEPARTMENTAL REPORTS, A SEMIFORMAL SERIES, RECORDING INFORMATION OF A PRELIMINARY OR TEMPORARY NATURE, OR OF LIMITED INTEREST OR SIGNIFICANCE, CARRYING A DEPARTMENTAL ALPHANUMERIC IDENTIFICATION.**
- (3) TECHNICAL MEMORANDA, AN INFORMAL SERIES, USUALLY INTERNAL WORKING PAPERS OR DIRECT REPORTS TO SPONSORS, NUMBERED AS TM SERIES REPORTS; NOT FOR GENERAL DISTRIBUTION.**

